

## Fabrication of novel ionic liquids-doped polyaniline as lubricant additive for anti-corrosion and tribological properties



Zhengfeng Cao<sup>a</sup>, Yanqiu Xia<sup>a,\*</sup>, Chuan Chen<sup>a,b</sup>

<sup>a</sup> School of Energy Power and Mechanical Engineering, North China Electric Power University, Beijing 102206, China

<sup>b</sup> Global Energy Interconnection Research Institute, Beijing 102206, China

### ARTICLE INFO

#### Keywords:

Polyaniline  
Ionic liquids  
Tribology  
Interfacial polymerization

### ABSTRACT

Two types of ionic liquids-doped polyaniline (ILs-doped PANI) were synthesized based on an improved interfacial polymerization and evaluated as anti-wear and anti-corrosion additives in poly alpha olefin (PAO) and polyurea grease. Their nanostructures and functionalization were analyzed in detail. The anti-corrosion performance of ILs-doped PANI was assessed via salt spray test, which reveals the excellent anti-corrosion performance. Tribological tests demonstrated that ILs-doped PANI as additives can remarkably reduce friction coefficients and wear volumes in PAO and also in polyurea grease. The scanning electron microscope (SEM) micrographs and X-ray photoelectron spectroscopy (XPS) spectra of the worn surfaces suggested the excellent friction reduction and anti-wear abilities of ILs-doped PANI were strongly dependent on the synergistic lubricating effect during the friction process.

### 1. Introduction

As the terminology is explained in mechanics, friction reflects the tangential movement resistance between two bodies in contact under the relative motion (or relative motion tendency) induced by external force, while the wear is the consequence of the friction. Friction is one of the most common physical phenomena which consumes a portion of energy, and the wear caused by friction is the main reason for the failure of mechanical devices [1–3]. To address the detrimental effects of friction and wear, lubricants and additives are generally employed to improve the friction reduction and anti-wear abilities. In the past decades, a lot of nanoparticles as potential lubricating additives have been experimentally evaluated through comparison analysis of the tribological behaviors [4–8]. Some nanoparticles have been successfully employed in mechanical equipment, thereby saving energy and creating a huge economic benefits.

Recently, polyaniline (PANI) as an ideal material has attracted our attention because of its excellent environmental stability, tunable conductivity, novel anti-corrosion property, controllable structure, as well as its easy preparation by chemical or electrochemical polymerization [9, 10]. We have reported that PANI as an additive in lubricating grease exhibited some certain friction reduction and anti-wear abilities under various conditions, and it also remarkably improved the anti-corrosion performance of the grease [11]. However, in our previous work, the

relatively large size of micro-PANI limited its tribological performances because nanoparticles generally exhibit better tribological properties than microparticles under boundary lubrication. Meanwhile, we found that micro-PANI as an additive in lubricating oil is easy to agglomerate and precipitate, which may result from its large size and the existence of a strong conjugated  $\pi$  electron system [12,13]. Therefore, in order to improve the tribological properties, it is of great significance to obtain nanometer PANI and improve its solubility. Some studies have reported that interfacial polymerization is a preferable approach to synthesize PANI in different nanostructures through controlling reaction parameters and reagents [13–16]. It is named as interfacial polymerization because the polymerization reaction is conducted at the interface of two immiscible solvents. Interfacial polymerization is a relatively easy method which has made it the preferable approach to synthesize conducting polymers [13–16]. To improve the solubility of PANI, various procedures have been adapted: (1) doping PANI by using the so-called functionalized protonic acids (such as dodecylbenzene-sulfonic or camphorsulfonic acid) in the protonation of PANI, resulting in enhanced solubility [17, 18]; (2) copolymerization or homopolymerization with aniline derivative (e.g. ring or N-substituted anilines) for improved solubility [19–21]; (3) incorporation of polar functional groups is a general approach to enhance solubility of PANI in common organic solvents and water [22, 23]. These previous studies provide a rich theoretical and experimental basis for the preparation of nanometer PANI with preferable solubility,

\* Corresponding author.

E-mail address: [xiayq@ncepu.edu.cn](mailto:xiayq@ncepu.edu.cn) (Y. Xia).

thus PANI could hold a great promise as a novel lubricant additive for a huge range of applications.

Room temperature ionic liquids (ILs) are organic salts, where inorganic/organic anions and organic cations are protected against to generate a common crystalline, thus maintaining the liquid phase at a wide range of temperature as the name describes. ILs have remarkable thermal stability, negligible vapor pressure and low volatility, which make it explored as promising green solvents [24,25]. Imidazolium-based ILs play an important part in the family of ILs. According to the previous studies, imidazolium-based ILs are sufficiently acidic in the 2-position, and the  $\pi$ - $\pi$  interaction and hydrogen bonding interaction could be generated between imidazolium ring and PANI [10, 26–28]. Therefore, imidazolium-based ILs are expected to serve as an unique dopant to afford protons for doping PANI and donate functional groups which can be incorporated onto PANI via  $\pi$ - $\pi$  interaction and hydrogen bonding interaction, resulting in enhanced solubility. Furthermore, due to the excellent anti-corrosion resistance of PANI and novel tribological properties of ILs [11–13,24,25], the functionalized PANI in association with imidazolium-based ILs may also exhibit an excellent anti-corrosion resistance and tribological behaviors.

In this work, two types of functionalized PANI in different nanostructures were synthesized based on an improved interfacial polymerization in which imidazolium-based ILs served as an organic phase to dissolve aniline monomers and dope PANI in the process of polymerization. This polymerization method also eliminated the usage of extra protonic acids. Meanwhile, compared with conventional interfacial polymerization, we also studied the possibility to synthesize PANI at the interface of two miscible phases. The nanostructures and functionalization of obtained ILs-doped PANI were characterized and analyzed by scanning electron microscope (SEM), energy dispersive X-ray spectroscopy (EDS) and Fourier transform infrared spectrometer (FT-IR), and the tribological performances, anti-corrosion property and lubrication mechanisms of obtained ILs-doped PANI as additives in lubricating oil and grease were investigated and discussed in detail.

## 2. Experimental section

### 2.1. Chemicals

1-butyl-3-methylimidazolium hexafluorophosphate (LP104, 99%) and 1-butyl-3-methylimidazolium tetrafluoroborate (LB104, 99%) were obtained from J&K Scientific Ltd (Beijing, China). Poly alpha olefin (PAO) as base oil was obtained from Golden Chemical Co., Ltd (Nanjing, China) and it has kinematic viscosity of 396 mm<sup>2</sup>/s at 40 °C and 39 mm<sup>2</sup>/s at 100 °C. Aniline, ammonium persulfate (APS) and acetone were all purchased from Sinopharm Chemical Reagent Co., Ltd (Shanghai, China) and they are all analytical reagent. Polyurea grease was provided by Zhongcheng Petrochemical Co., Ltd (Changsha, China).

### 2.2. Synthesis and characterization of ILs-doped PANI

The ILs-doped PANI were synthesized as following steps. First, 10 g of ILs containing 0.4 g aniline and 10 g of distilled water containing 0.98 g APS were efficiently dispersed for 10 min by ultrasonic wave, respectively. Second, the APS aqueous solution was slowly transferred into the breaker of aniline-ILs solution. After 10 min, PANI was generated at the interface of ILs and distilled water. With no disturbance, the reaction lasted for 24 h at room temperature. Finally, the mixture was filtered and washed with acetone and distilled water for several times, and then the filtrate cakes were dried using a heat oven at 40 °C and for 12 h to obtain the ILs-doped PANI (were abbreviated as PANI-LP104 and PANI-LB104).

A SU8010 scanning electron microscope (SEM, Hitachi) was employed to take micrographs of PANI-LP104 and PANI-LB104. A Fourier transform infrared (FT-IR) spectrometer (Thermo Fisher Scientific) recorded the FT-IR spectra of LP104, LB104, PANI-LP104 and PANI-LB104 in the wavenumber range of 4000–400 cm<sup>-1</sup>. And an EVO-18

scanning electron microscope-energy dispersive X-ray spectroscopy (SEM-EDS) (Zeiss SEM, Bruker EDS) was employed to characterize the chemical compositions of ILs-doped PANI under 12 kv accelerating voltage with 7.5 nm beam current.

### 2.3. Tribological characterization

#### 2.3.1. Lubricant preparation

The lubricants were obtained by mixing the PAO/polyurea greases and additives thoroughly via vigorous stirring for 30 min at room temperature. It was found that no precipitate was observed in the lubricating oil after a storage for 24 h, indicating a preferable dispersion and stability of ILs-doped PANI in the base oil. Furthermore, the lubricating greases need to be grinded using a three-roller mill to ensure uniform dispersion of the additives. The concentration of additives in PAO and polyurea greases was adjusted as 0.1%, 0.2%, 0.3% and 0.4% (mass fraction). The LB104 was also added into base oil and grease to prepare lubricants.

#### 2.3.2. Friction and wear test

The tribological properties of lubricants for steel/steel pair were evaluated on a MFT-R4000 reciprocal friction and wear tester with a ball-on-disc configuration, which was provided by State Key Laboratory of Solid Lubrication, Lanzhou Institute of Chemical Physics, Chinese Academy of Science (Lanzhou, China). The upper ball (AISI 52100 steel ball, diameter 5 mm, hardness 710 Hv) slides reciprocally against the fixed lower disc ( $\Phi$ 24 mm  $\times$  7.9 mm, AISI 52100 steel, hardness 590–610 Hv, surface roughness 0.05  $\mu$ m) at a stroke of 5 mm, a frequency of 5 Hz and a normal load of 50–200 N (corresponding to the Hertzian pressure in the range of 1.7–2.7 GPa) for a duration of 30 min at room temperature (RT). Before and after every tribological test, the running balls and lower discs were cleaned in acetone for 10 min utilizing an ultrasonic cleaner. Prior to test, about 0.5 g lubricant was introduced into the sliding region and every friction and wear test was conducted thrice to get more reliable values. A computer noted down the coefficient of friction (COF) and a Micro-XAM 3D surface mapping microscopy profile meter determined the wear volumes on the steel discs.

### 2.4. Corrosion test

The anti-corrosion property of the lubricating greases were evaluated via salt spray test according to the ASTM B117. Some bright finish steel blocks were evenly coated with lubricating greases, and then placed in a salt spray test chamber under the temperature of 35  $\pm$  1 °C and the NaCl concentration of 5  $\pm$  0.1% for a duration of 720 h. After that, the steel blocks were washed with acetone and thoroughly air-dried, and a PHI-5702 multifunctional X-ray photoelectron spectroscopy (XPS, American Institute of Physics Electronics Company) with K-alpha irradiation as the excitation source was employed to analyze the chemical states of characteristics elements on the steel block surfaces. A pass energy of 29.3 eV characterized the binding energies of the target elements with the binding energy of carbon (C1s: 284.6 eV) as the reference.

### 2.5. Surface characterization

After tribological test, the steel discs were ultrasonically cleaned with acetone for 10 min. An EVO-18 SEM (Zeiss, Germany) was employed to take the images of the wear scars and an XPS was employed to analyze the chemical states of the characteristics elements on the rubbing surfaces. The test parameters were the same as that mentioned above.

## 3. Result

### 3.1. Analysis of ILs-doped polyaniline

In general, interfacial polymerization involves that two reactive

agents are dissolved respectively in two immiscible solvents, and target product is generated at the interface of the two immiscible phases [13–16]. As is known to all, water cannot be mutually soluble with LP104, but with LB104. Therefore, PANI could be synthesized normally at the interface of water and LP104. In terms of the system composed of water and LB104, although they were miscible, we found that an interface was still successfully formed between water and LB104 and maintained for at least 24 h. Here, density may make a great contribution for the formation of the interface because the larger density of LB104 keeps LB104 staying in the bottom of the breaker for a long duration during the polymerization (LB104: 1.26 g/cm<sup>3</sup>, 25 °C; water: 1 g/cm<sup>3</sup>, 25 °C). Thus, two types of ILS-doped PANI were successfully fabricated based on interfacial polymerization and their structures, FT-IR and chemical compositions were characterized and discussed in following sections.

Fig. 1 presents the SEM morphologies of the PANI-LP104 and PANI-LB104. Observing the images, two types of ILS-doped PANI show different shapes, where PANI-LP104 is rod-shaped with the diameter of about 100 nm but PANI-LB104 shows an irregular shape. In the course of interfacial polymerization, PANI is generated at the interface of water and ILS and then moves into water phase because the amino groups located at the end of PANI chains are hydrophilic. At the interface between water and LB104, a relatively thick film (reaction region) may be formed because of the mutual solubility of water and LB104, so that PANI stayed in the reaction region for a relatively long time, resulting in a large nucleation amount and secondary growth, which is responsible for the irregular shape of PANI-LB104.

Fig. 2 shows the FT-IR spectra of the ILS and PANI to confirm the presence of functional groups of ILS on PANI. As shown in Fig. 2(a), the characteristics peaks at 1064 and 839 cm<sup>-1</sup> are attributed to the B-F stretching vibration and P-F stretching vibration from the anions, respectively. The peaks located at 1565 and 1474 cm<sup>-1</sup> belong to the C-N bands on the imidazolium ring [24,26,29]. The peaks at 3170 and 2960 cm<sup>-1</sup> are assigned to the H-C-C-H asymmetric stretch and N=C stretch vibrations on imidazolium rings [30]. Observing the Fig. 2(b), the ILS-doped PANI exhibit the characteristics peaks at 1567 and 1479 cm<sup>-1</sup>, belonging to the C=C stretching vibration of quinoid and benzenoid rings, respectively. The peaks located at 1305 and 1242 cm<sup>-1</sup> are assigned to C-N stretching vibration for the benzenoid unit, and the peaks located at 1112 cm<sup>-1</sup> belongs to the in-plane bending vibration of C-H [9,30,31]. The relatively ratio of quinoid to benzenoid ring can be calculated approximately on the basis of the intensity ratio of the peaks at 1567 and 1479 cm<sup>-1</sup>. When the ratio of benzenoid to quinoid rings is larger than 1.0, PANI was protonated [31]. Thus, it can be determined from FT-IR spectra that the ILS-doped PANI had been successfully doped with protons. In the region between 2500 and 400 cm<sup>-1</sup> of FT-IR spectra, it is difficult to determine whether the functional groups of ILS are present on the PANI because the peaks of ILS are almost overlapped by the peaks of PANI. However, observing the region above 2500 cm<sup>-1</sup>, the characteristics peaks on the FT-IR spectra of ILS-doped PANI located at 3170 and 2960 cm<sup>-1</sup> are attributed to the imidazolium ring [26], which proves a successful modification of PANI with functional groups of

imidazolium-based ILS.

Fig. 3 presents the EDS elemental surface distribution images of the PANI-LP104 and PANI-LB104 to provide a direct evidence for the successful modification. Observing the images, the typical elements including F, B and P have reached high-density coverage on the obtained PANI, which further proves that the PANI were modified effectively with ILS via  $\pi$ - $\pi$  interaction and hydrogen bonding interaction during the polymerization of aniline monomers.

### 3.2. Tribological properties of ILS-doped PANI as additives in PAO

Fig. 4 shows the COFs and wear volumes for steel/steel contact as a function of the adding amount of PANI-LP104 and PANI-LB104 in PAO at 50 N, 5 Hz and RT. It is visible that the overall COFs and wear volumes decrease first and then increase as the additive concentration increases. The reason is ascribed that the tribological performances of solid lubricant additives depend on the optimal concentration because low concentration is not capable to form a sufficient tribofilm but high concentration may cause agglomeration and abrasive wear. The results show that the most significant improvement for lubricity of PANI-LP104 and PANI-LB104 is obtained by the PAO with the same concentration of 0.2 wt% ILS-doped PANI.

Fig. 5 presents the friction reduction and anti-wear abilities of different additives in PAO at various loads, 5 Hz and RT. As shown in Fig. 5(a), PANI-LP104 and PANI-LB104 have close COFs which are all lower than that of pure PAO and PAO+0.2 wt% LB104 at different loads, indicating ILS-doped PANI have preferable friction reduction property in PAO. Fig. 5(b) shows that the addition of PANI-LP104 and PAN-LB104 can reduce the wear volumes by several times at different loads as compared to pure PAO, indicating an excellent anti-wear property. The excellent tribological behaviors may be attributed to that the ILS-doped PANI can easily adsorb on the rubbing surfaces to decrease close contact between the friction interfaces and form a protective tribofilm throughout the sliding process.

SEM was employed to obtain the morphologies of worn surfaces after friction test to further compare the tribological performances of different lubricants. Fig. 6 displays the SEM morphologies of worn surfaces on the steel discs lubricated by PAO and PAO plus 0.2 wt% each of different additives at 200 N, 5 Hz and RT. As shown in Fig. 6(a-d), the steel discs lubricated by PAO and PAO+LB104 acquire considerably wider and deeper wear scars and a lot of deep and narrow furrows appear on the worn surfaces, indicating severe scuffing occur in this condition. As shown in Fig. 6(e-h), the addition of PANI-LP104 and PANI-LB104 remarkably reduced the wear widths and made the surfaces became smoother, implying ILS-doped PANI have an excellent anti-wear ability.

### 3.3. Tribological properties of ILS-doped PANI as additives in polyurea grease

Polyurea grease has attracted considerable research and extensive applications owing to its novel anti-oxidation, wide range of operating

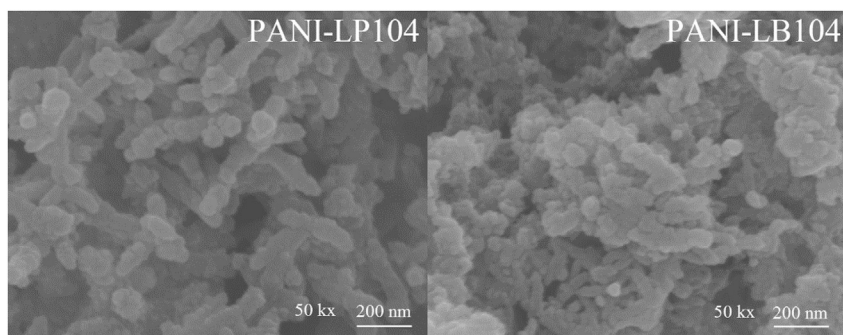


Fig. 1. SEM morphologies of PANI-LP104 and PANI-LB104.

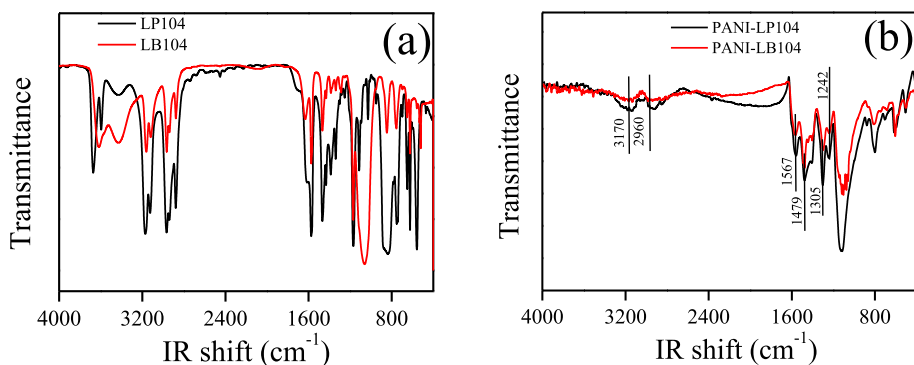


Fig. 2. FT-IR spectra of (a) ILS and (b) ILS-doped PANI.

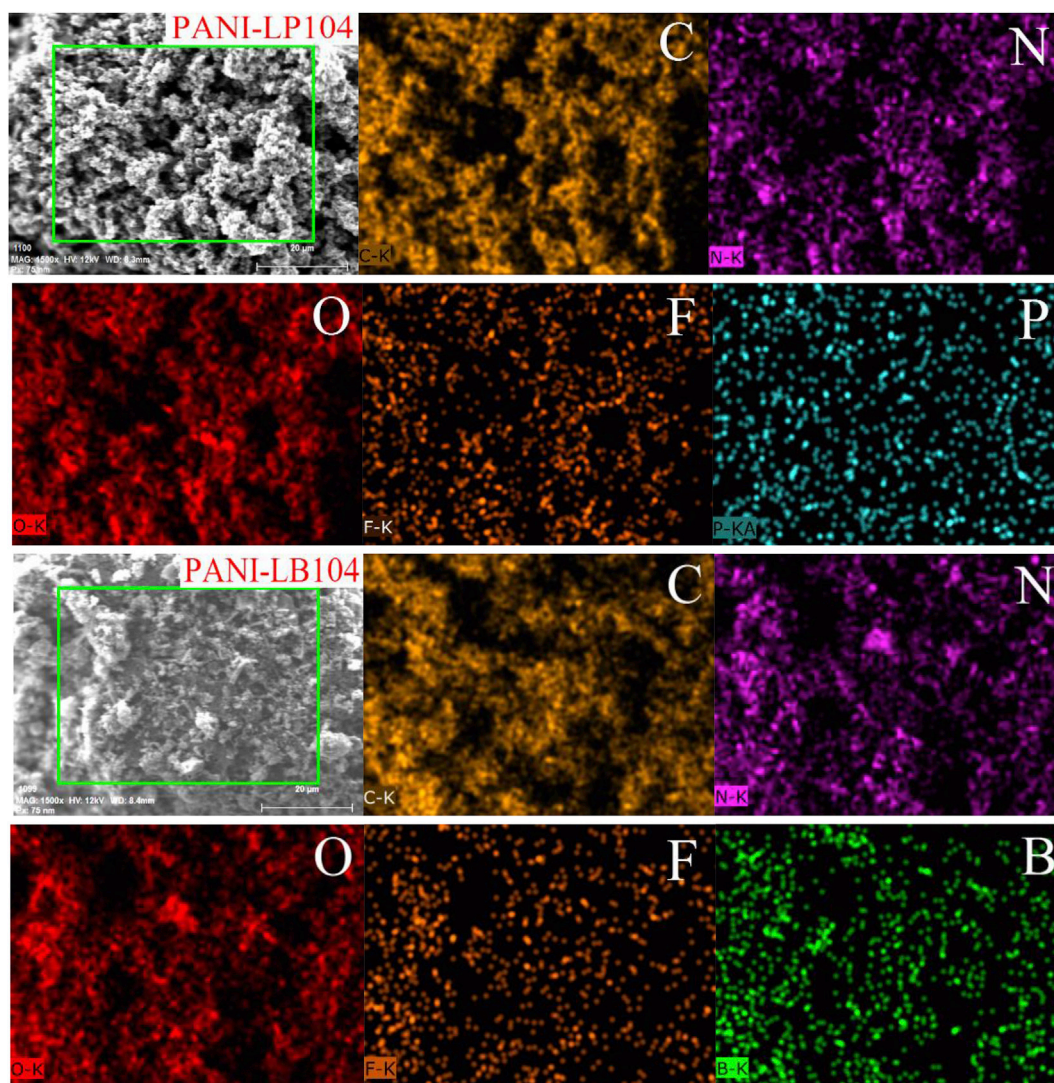


Fig. 3. EDS elemental surface distribution images of the PANI-LP104 and PANI-LB104.

temperature, remarkable thermal, mechanical and colloidal stabilities [32–34]. Therefore, we continued to investigate the effect of PANI-LP104 and PANI-LB104 on the tribological performances of polyurea grease.

Fig. 7 shows the COFs and wear volumes for polyurea grease in the absence and presence of different ILS-doped PANI concentrations at 50 N, 5 Hz and RT. It can be seen that the ILS-doped PANI at different concentrations all can remarkably lower the COFs and wear volumes. The PANI-LP104 shows better friction reduction and anti-wear abilities than

PANI-LB104, which may be ascribed to that the  $PF_4^-$  anion has a more active property than  $BF_4^-$ , leading to that PANI-LP104 can more easily adsorb on the worn surfaces and react with metal to form a protective film. Taking into account the friction reduction and anti-wear abilities, the optimal concentration of ILS-doped PANI in polyurea grease is determined as 0.3 wt% to provide excellent tribological performances.

Fig. 8 displays the COFs and wear volumes for polyurea grease in the absence and presence of different additives at various loads, 5 Hz and RT.

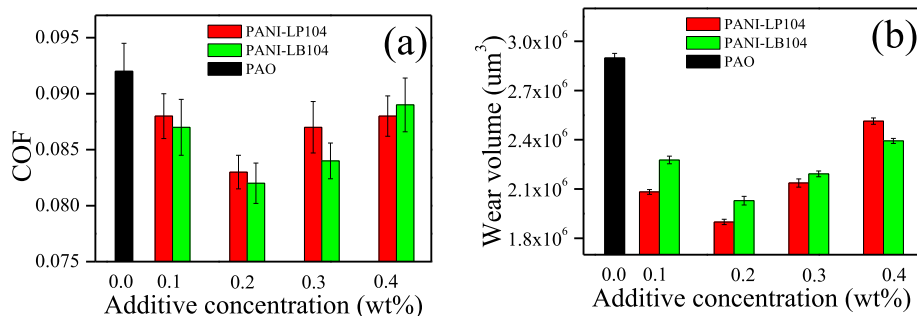


Fig. 4. COFs (a) and wear volumes (b) for PAO plus different concentrations of ILS-doped PANI at 50 N, 5 Hz and RT.

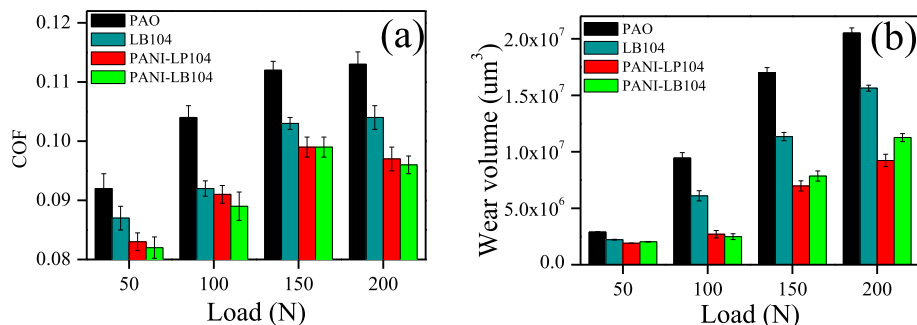


Fig. 5. COFs (a) and wear volumes (b) for PAO and PAO plus 0.2 wt% each of different additives at various loads, 5 Hz and RT.

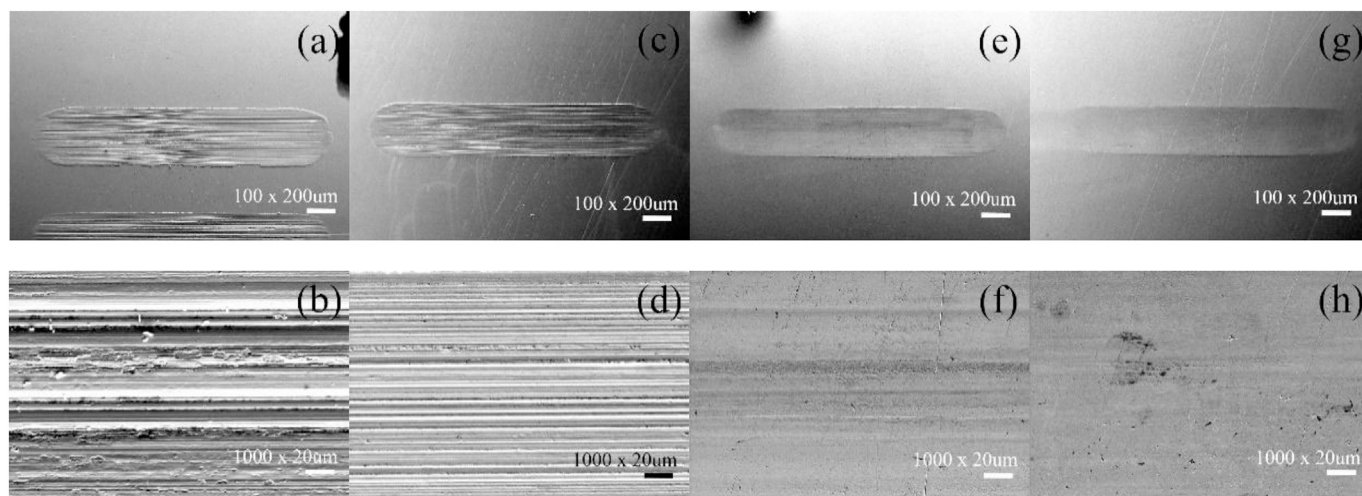


Fig. 6. SEM morphologies of worn surfaces on steel discs lubricated by (a-b) PAO, (c-d) LB104, (e-f) PANI-LP104, (g-h) PANI-LB104 at 200 N, 5 Hz and RT.

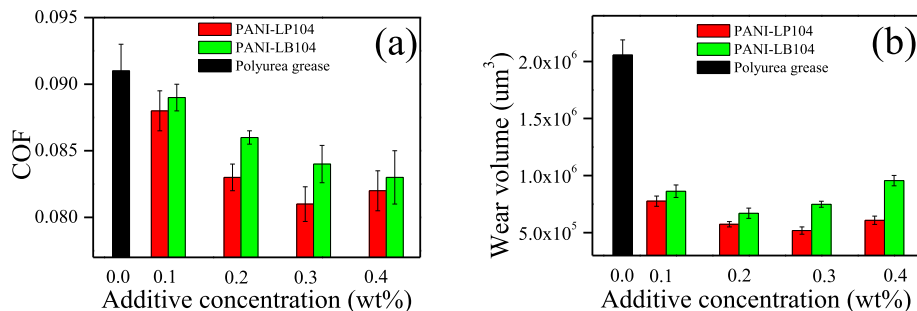


Fig. 7. COFs (a) and wear volumes (b) for polyurea grease plus different concentration of ILS-doped PANI at 50 N, 5 Hz and RT.

As shown in Fig. 8, although overall trends of the COFs and wear volumes of lubricating greases increase with the normal load ranging from 50 to

200 N, the values of PANI-LP104 and PANI-LB104 are still lower than others. When the load is 200 N, PANI-LP104 and PANI-LB104 reduce the

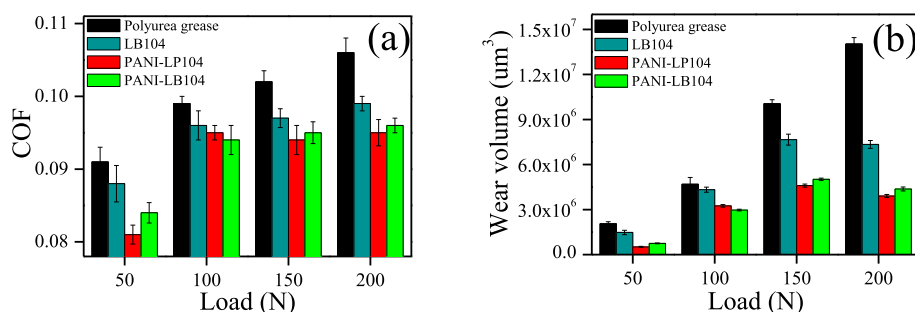


Fig. 8. COFs (a) and wear volumes (b) for polyurea grease and polyurea grease plus 0.3 wt% each of different additives at various loads, 5 Hz and RT.

wear volumes by 3.6 and 3.2 times as compared with polyurea grease, respectively. This results reveal that PANI-LP104 and PANI-LB104 as additives in polyurea grease can also remarkably improve the friction reduction and anti-wear abilities at different loads.

Fig. 9 displays the SEM morphologies of the worn surfaces on the steel discs lubricated by different lubricating greases at 200 N, 5 Hz and RT. As shown in Fig. 9(a-b), although polyurea grease has a good friction reduction and anti-wear abilities, the wear surface acquires a relatively wide wear scar and rough friction surface with some narrow and deep grooves. Fig. 9(c-d) shows a little narrow wear scar and smooth worn surface, indicating the addition of 0.3 wt% LB104 in polyurea grease exhibits come certain anti-wear ability. Observing the Fig. 9(e-h), it is visible that the addition of PANI-LP104 and PANI-LB104 not only significantly reduce the wear widths, but also greatly make the worn surfaces become smoother, which reveals that PANI-LP104 and PANI-LB104 as additives in polyurea grease exhibit excellent anti-wear ability.

### 3.4. Salt spray corrosion test

The steel blocks after salt spray test were washed with acetone and Fig. 10 shows the pictures. The blocks (Fig. 10(c-d)) covered with the greases in the presence of PANI-LP104 and PANI-LB104 were bright as compared with pure polyurea grease, indicating ILS-doped PANI as additives in polyurea greases exhibited an excellent anti-corrosion property. The block covered with LB104 grease acquired many corrosion spots because LB104 has corrosion property [32,35]. The anti-corrosion mechanisms is explained in the discussion sections.

### 3.5. XPS analysis of worn surfaces

Since XPS as a powerful facility could offer the information about the

chemical states of characteristics elements on the worn surfaces, therefore, it is usually employed to probe the lubrication mechanisms. Fig. 11(a-f) gives the XPS spectra of Fe2p, O1s, F1s, B1s, N1s and P2p on the worn surfaces lubricated by PAO in absence and presence of different additives. XPS Fe2p spectra at 724.3 eV and 710.8 eV may correspond to Fe<sub>2</sub>O<sub>3</sub> and Fe<sub>3</sub>O<sub>4</sub> [34,35]. The peaks of O1s located at 530.0–531.5 eV may be ascribed to FeO and C-O compounds, implying the formation of complex oxide species [32,34,35]. The peaks of F1s at 684.5 eV may belong to FeF<sub>2</sub> and FeF<sub>3</sub>, and another peak located at 689.0 eV may belong to C-F binding [36,37]. The generation of borides is uncertain because the characteristics peak of B1s was not detected on the worn surfaces. The binding energies of N1s appearing at about 400.2 eV may belong to carbonitride and/or nitrogen oxide, and/or nitrogen doubled-bond compounds [32,35]. The peak of P2p at 133.5 eV may illustrate the presence of FePO<sub>4</sub> [38,39]. XPS analysis suggests that a protective lubrication film was generated on the worn surfaces by complex physical adsorption and tribo-chemical reactions, which was responsible for the enhanced friction reduction and anti-wear abilities throughout the friction process.

## 4. Discussion

### 4.1. The unique functions of ILS during the polymerization

Two types of ILS-doped PANI in nanostructures have been successfully fabricated at the interface of water and imidazolium-based ILS. In the process of interfacial polymerization, the imidazolium-based ILS perform multiple functions which can be described as following aspects: (1) ILS, even the water-miscible LB104, work as a liquid phase to dissolve aniline monomers in the polymerization. Meanwhile, the mutual solubility between ILS and water could have a significant influence on the structures

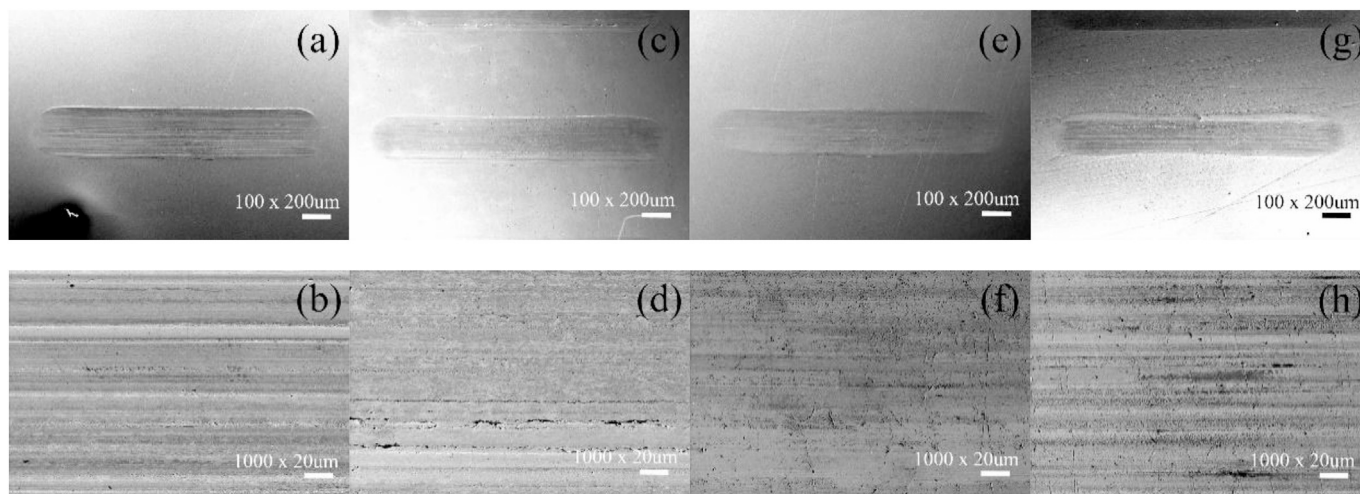


Fig. 9. SEM morphologies of the worn surfaces on steel discs lubricated by (a-b) polyurea grease, (c-d) LB104, (e-f) PANI-LP104, (g-h) PANI-LB104 at 200 N, 5 Hz and RT.

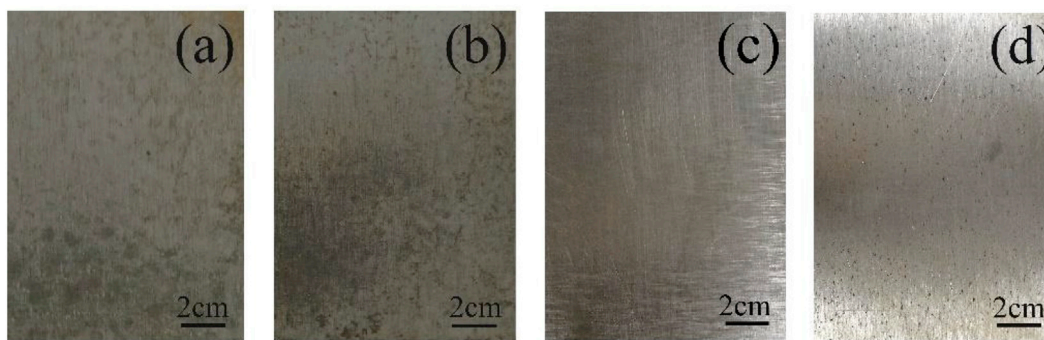


Fig. 10. Pictures of steel blocks after salt spray test. (a) polyurea grease, (b) LB104 grease, (c) PANI-LP104 grease and (d) PANI-LB104 grease.

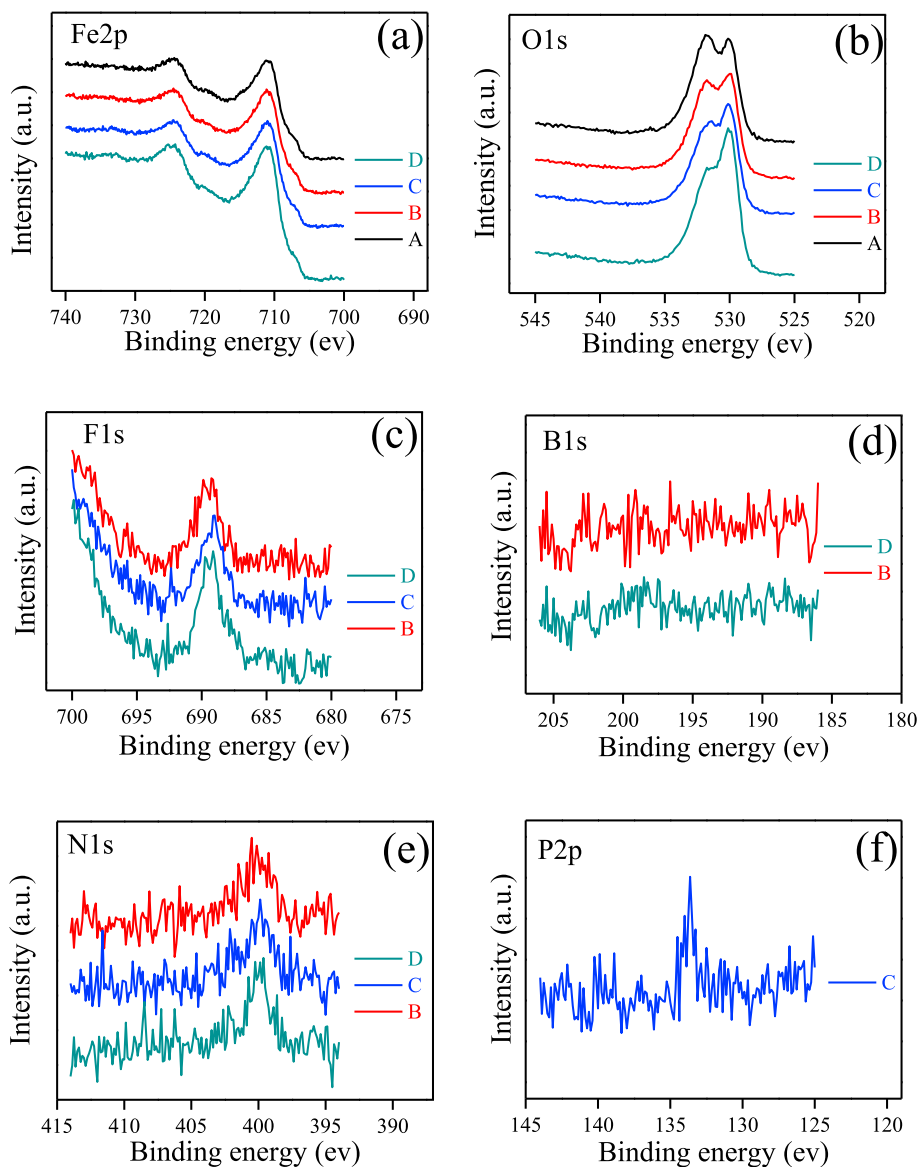


Fig. 11. XPS spectra of (a) Fe2p, (b) O1s, (c) F1s, (d) B1s, (e) N1s and (f) P2p on the worn surfaces lubricated by (A) PAO, (B) PAO+LB104, (C) PAO+PANI-LP104 and (D) PAO+PANI-LB104.

of obtained PANI. (2) Because imidazolium-based ILs are sufficiently acidic in the 2-position, ILs act as functional acids to protonate the PANI, resulting improved solubility, conductivity and anti-corrosion

performance [10,17,18,26–28]. Meanwhile, compared with conventional interfacial polymerization of PANI, this approach eliminates the usage of extra protonic acids as dopant. (3) Imidazolium-based ILs serve

as unique dopant to modify PANI via hydrogen bonding interaction and  $\pi$ - $\pi$  interaction for enhanced solubility and tribological properties [10,22,23,26,28].

#### 4.2. Anti-corrosion mechanism of PANI in lubricating greases

Salt spray test indicates lubricating greases containing ILS-doped PANI have preferable anti-corrosion ability. Wessling and Fahlman proposed the passivation mechanism of PANI for the excellent anti-corrosion ability through an XPS study [40,41], and it has been thoroughly studied and proved in recent decades [42–46]. Here, two rational mechanisms may be responsible for the excellent anti-corrosion performance of the lubricating greases. (1) Physical barrier effect. The lubricating greases work as a barrier to protect the substrate metals against the invasion of corrosive substances. (2) Passivation mechanisms. In salt spray test, the corrosion potential of bare steel is usually located in the active potential region and the corrosion rate is relatively high. Since PANI has a higher potential than substrate steel, therefore, it could work as an oxidant to shift the potential of steel in the passive region. Thus, a dense passivation film composed of iron oxides is formed on the metal surface, leading to a reduction in corrosion rate of steel [42–46]. To support this anti-corrosion mechanisms, the steel block surfaces were characterized by the XPS and Fig. 12 gives the XPS spectra of Fe2p and O1s on the steel block surfaces covered by the greases in the absence and presence of ILS-doped PANI after salt spray test.

As shown in Fig. 12, the peaks of Fe2p at about 710.5 and 724.1 eV belong to  $\text{Fe}_2\text{O}_3$  and  $\text{Fe}_3\text{O}_4$ , respectively, and the peaks of O1s at about 529.6 and 531.3 eV suggest the generation of iron oxide. The Fe2p and O1s on the surface covered by polyurea grease also exhibit relatively strong peaks at 724.1 and 531.3 eV as compared with the Fe2p and O1s on the surfaces covered by greases containing ILS-doped PANI, which is attributed to that the steel blocks covered by polyurea grease was corroded during the salt spray test. The XPS spectra of Fe2p on the surfaces covered by greases containing ILS-doped PANI are similar to the results described by Fahlman and Wessling in their works where the Fe2p protected by PANI exhibited relatively weak peaks at about 724.1 eV and the peaks are slightly shifted to high binding energy, indicating that a passivation film composed of iron oxide was generated on the worn surfaces for corrosion prevention [40,41].

#### 4.3. Lubrication mechanisms of ILS-doped PANI as additives

Functionalized PANI is presented as an ideal material for enhanced tribological properties and its preferable friction reduction and anti-wear abilities have been proved based on the tribological tests and SEM analysis. The results inspire us to further explore the lubrication mechanisms. Herein, the lubrication mechanisms may be explained by two aspects.

- (1) It is well-known that nanoparticles such as carbon nanotubes, graphene and nano-Cu can fill the valley of surfaces to avoid the direct contact and achieve the rolling/sliding functions by acting as spacers or bearings between the contact pairs, thereby forming an easily shearing film on the rubbing surfaces for enhanced tribological performances [2,24,29,47–49]. Herein, the synthesized ILS-doped PANI as nanometer materials may perform similar functions for the excellent friction reduction and anti-wear abilities.
- (2) XPS offers some information about the lubrication mechanisms. Keeping eyes on the XPS spectra shown in Fig. 11, the binding energies of the Fe, O, F, B and N are similar on the rubbing surfaces lubricated by PANI-LP104, PANI-LB104 and LB104, indicating they experienced similar tribo-chemical reaction throughout the friction process. XPS analysis suggests that the functional groups of ILS on PANI-LP104 and PANI-LB104 may make a great contribution for the formation of the protective film which is composed of  $\text{FeO}$ ,  $\text{Fe}_2\text{O}_3$ ,  $\text{Fe}_3\text{O}_4$ ,  $\text{FeF}_2$ ,  $\text{FeF}_3$  or  $\text{FePO}_4$  during the friction process. The binding energy of N1s located at 400.2 eV corresponds to carbonitride and/or nitrogen oxide, and/or nitrogen doubled-bond compounds [32,35]. It may be an evidence for the physical adsorption film generated by ILS-doped PANI. In addition, nanometer particles modified with ILS could have an improved stability in lubricants [24,29,50], which also benefits the tribological performances.

Consequently, based on the characterization and analysis of ILS-doped PANI, and the SEM and XPS analysis of worn surfaces, the excellent friction reduction and anti-wear abilities mainly depend on the synergistic lubricating effect of the rolling/sliding functions and the physical adsorption film and the tribo-chemical reaction film on the worn surfaces. Hence, the ILS-doped PANI as an ideal material holds a great potential for a wide range of applications.

## 5. Conclusions

We summarize the abovementioned experimental results and analysis as follow: the ILS-doped PANI including PANI-LP104 and PANI-LB104 were successfully synthesized based on the improved interfacial polymerization. SEM micrographs showed that PANI-LP104 was rod-shaped with the diameter of about 100 nm and PANI-LB104 was irregular shaped. SEM-EDS and FT-IR analysis showed that both of obtained PANI were effectively doped with imidazolium-based ILS via  $\pi$ - $\pi$  interaction and hydrogen bonding interaction in the process of polymerization. Salt spray test suggested that ILS-doped PANI as additives in polyurea grease exhibited excellent anti-corrosion performance, which depended on the physical barrier effect and passivation mechanisms. In addition, PAO containing 0.2 wt% ILS-doped PANI and polyurea greases containing 0.3 wt% ILS-doped PANI exhibited excellent friction reduction and anti-wear abilities under a series of friction tests as compared to pure PAO/

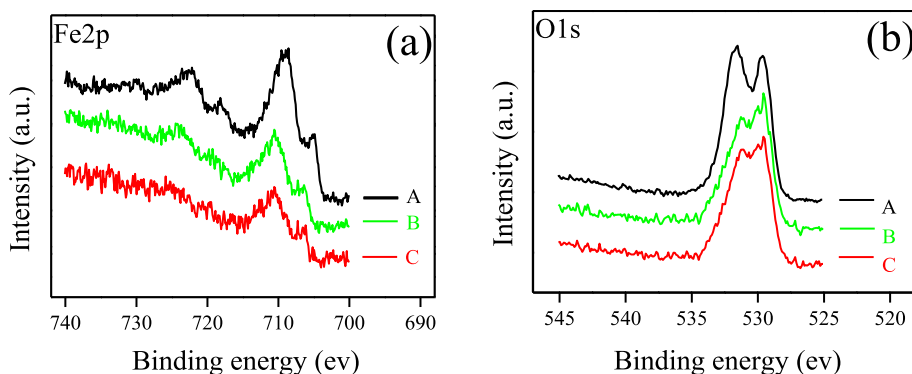


Fig. 12. XPS spectra of (a) Fe2p and (b) O1s on the steel block surfaces covered by (A) polyurea grease, (B) PANI-LP104 grease and (C) PANI-LB104 grease after salt spray test.

polyurea grease and lubricants adding LB104. Based on the SEM and XPS analysis, the excellent tribological properties are ascribed to the synergistic lubricating effect because ILS-doped PANI could avoid the direct contact between the friction interfaces and generate physical adsorption film and tribo-chemical reaction film on the worn surfaces throughout the friction process. Given the simple and effective synthetic approach, the excellent anti-corrosion performance and tribological properties, ILS-doped PANI as an ideal material holds a great potential for a huge applications in lubrication domain.

## Acknowledgements

This work is supported by the National Natural Science Foundation of China (Grant 51575181) and Natural Science Foundation of Beijing Municipality (Grant 2172053).

## References

- Liu L, Zhou W. MoS<sub>2</sub> hollow microspheres used as a green lubricating additive for liquid paraffin. *Tribol Int* 2017;114:315–21.
- Fan XQ, Li W, Fu HM, Zhu MH, Wang LP, Cai ZB, et al. Probing the function of solid nanoparticle structure under boundary lubrication. *ACS Sustain Chem Eng* 2017; 5(5):4223–33.
- Matta C, Jolyptottuz L, De BBMI, Martin JM, Kano M, Zhang Q, et al. Superlubricity and tribochemistry of polyhydric alcohols. *Phys Rev B* 2008;78(8), 085436.
- Zhang XF, Luster B, Church A, Muratore C, Voevodin AA, Kohli P, et al. Carbon nanotube-MoS<sub>2</sub> composites as solid lubricants. *ACS Appl Mater Inter* 2009;1(3): 735–9.
- Fan XQ, Wang LP, Li W, Wan SH. Improving tribological properties of multialkylated cyclopentanes under simulated space environment: two feasible approaches. *ACS Appl Mater Inter* 2015;7(26):14359–68.
- Sharma V, Timmons R, Erdemir A, Aswath PB. Plasma functionalized PTFE nanoparticles for improved wear in lubricated contact. *ACS Appl Mater Inter* 2017; 9(30):25631–41.
- Wu YY, Tsui WC, Liu TC. Experimental analysis of tribological properties of lubricating oils with nanoparticle additives. *Wear* 2007;262(7–8):819–25.
- Hu ZS, Dong JX, Chen GX, He JZ. Preparation and tribological properties of nanoparticle lanthanum borate. *Wear* 2000;243(1–2):43–7.
- Gu Y, Tsai JY. Enzymatic synthesis of conductive polyaniline in the presence of ionic liquid. *Synth Met* 2012;161(23–24):2743–7.
- Qu K, Zeng X. Ionic liquid-doped polyaniline and its redox activities in the zwitterionic biological buffer MOPS. *Electrochim Acta* 2016;202:73–83.
- Cao ZF, Xia YQ. Corrosion resistance and tribological characteristics of polyaniline as lubricating additive in grease. *J Tribol-T-ASME* 2017;139(6), 061801.
- Jaymand M. Recent progress in chemical modification of polyaniline. *Prog Polym Sci* 2013;38(9):1287–306.
- Bhadra S, Khastgir D, Singha NK, Lee JH. Progress in preparation, processing and applications of polyaniline. *Prog Polym Sci* 2009;34(8):783–810.
- Gao HX, Jiang T, Han BX, Wang Y, Du JM, Liu ZM, et al. Aqueous/Ionic liquid interfacial polymerization for preparing polyaniline nanoparticles. *Polymer* 2004; 45(9):3017–9.
- Dallas P, Stamopoulos D, Boukos N, Tzitzios V, Niarchos D, Petridis D. Characterization, magnetic and transport properties of polyaniline synthesized through interfacial polymerization. *Polymer* 2007;48(11):3162–9.
- Chen J, Chao D, Lu X, Zhang W. Novel interfacial polymerization for radially oriented polyaniline nanofibers. *Mater Lett* 2007;61(6):1419–23.
- Athawale AA, Kulkarni MV, Chabukswar VV. Studies on chemically synthesized soluble acrylic acid doped polyaniline. *Mater Chem Phys* 2002;73(1):106–10.
- Wang CC, Song JF, Bao HM, Shen QD, Yang CZ. Enhancement of electrical properties of ferroelectric polymers by polyaniline nanofibers with controllable conductivities. *Adv Funct Mater* 2010;18(8):1299–306.
- Saini P, Choudhary V. Structural details, electrical properties, and electromagnetic interference shielding response of processable copolymers of aniline. *J Mater Sci* 2013;48(2):797–804.
- Grigoras M, Catargiu AM, Tudorache F, Dobromir M. Chemical synthesis and characterization of self-doped N-propanesulfonic acid polyaniline derivatives. *Iran Polym J* 2012;21(2):131–41.
- Mu S. Synthesis and electronic properties of poly(aniline-co-2-amino-4-hydroxybenzenesulfonic acid). *J Phys Chem B* 2008;112(20):6344–9.
- Teh CH, Rozaidi R, Rusli D, Sahrim HA. Synthesis and spectroscopic studies of DGEBA-grafted polyaniline. *Polym-Plast Technol Eng* 2008;48(1):17–24.
- Takuma Y, Isao Y, Takakazu Y. Preparation of N-grafted polyanilines with oligoether side chains by using ping-opening graft copolymerization of epoxide, and their optical, electrochemical and thermal properties and ionic conductivity. *J Mater Chem* 2003;13(9):2138–44.
- Fu HM, Fan XQ, Li W, Zhu MH, Peng JF, Li H. In situ modified multilayer graphene toward high-performance lubricating additive. *RSC Adv* 2017;7(39):24399–409.
- Sanes J, Carrión FJ, Bermúdez MD, Martínez-Nicolás G. Ionic liquids as lubricants of polystyrene and polyamide 6-steel contacts. Preparation and properties of new polymer-ionic liquid dispersions. *Tribol Lett* 2006;21(2):121–33.
- Stejskal J, Dybal J, Trchová M. The material combining conducting polymer and ionic liquid: hydrogen bonding interactions between polyaniline and imidazolium salt. *Synth Met* 2014;197(197):168–74.
- Zhao F, Wang M, Ma Y, Zeng B. Electrochemical preparation of polyaniline-ionic liquid based solid phase microextraction fiber and its application in the determination of benzene derivatives. *J Chromatogr A* 2011;1218(3):387–91.
- Fabio R, Do NGM, Santos PS. Dissolution and doping of polyaniline emeraldine base in imidazolium ionic liquids investigated by spectroscopic techniques. *Macromol Rapid Comm* 2010;28(5):666–9.
- Fan XQ, Wang LP. High-performance lubricant additives based on modified graphene oxide by ionic liquids. *J Colloid Interface Sci* 2015;452:98–108.
- Leng C, Wei J, Liu Z, Shi J. Influence of imidazolium-based ionic liquids on the performance of polyaniline-CoFe<sub>2</sub>O<sub>4</sub> nanocomposites. *J Alloy Comp* 2011;509(6): 3052–6.
- Tian F, Qin ZY, Wu Q, Lu YQ. Effects of reaction conditions on microstructures and properties of polyaniline nanofibers through interfacial polymerization. *Adv Mater Res* 2013;750–752:293–6.
- Cai MR, Liang YM, Zhou F, Liu WM. Tribological properties of novel imidazolium ionic liquids bearing benzotriazole group as the antiwear/anticorrosion additive in poly(ethylene glycol) and polyurea grease for steel/steel contacts. *ACS Appl Mater Inter* 2011;3(12):4580–92.
- Sheth JP, Yilgor E, Erenturk B, Ozhalici H, Yilgor I, Wilkes GL. Structure–property behavior of poly(dimethylsiloxane) based segmented polyurea copolymers modified with poly(propylene oxide). *Polymer* 2005;46(19):8185–93.
- Cai MR, Zhao Z, Liang YM, Zhou F, Liu WM. Alkyl imidazolium ionic liquids as friction reduction and anti-wear additive in polyurea grease for steel/steel contacts. *Tribol Lett* 2010;40(2):215–24.
- Cai MR, Liang YM, Zhou F, Liu WM. A novel imidazolium salt with antioxidation and anticorrosion dual functionalities as the additive in poly(ethylene glycol) for steel/steel contacts. *Wear* 2013;306(1–2):197–208.
- Minami I. Ionic liquids in tribology. *Molecules* 2009;14(6):2286–305.
- Jiménez AE, Bermúdez MD, Iglesias P, Carrión FJ, Martínez-Nicolás G. 1-N-alkyl-3-methylimidazolium ionic liquids as neat lubricants and lubricant additives in steel-aluminium contacts. *Wear* 2006;260(7–8):766–82.
- Fan XQ, Xia YQ, Wang LP. Tribological properties of conductive lubricating greases. *Friction* 2014;2(4):343–53.
- Wang H, Lu Q, Ye C, Cui Z. Friction and wear behaviors of ionic liquid of alkylimidazolium hexafluorophosphates as lubricants for steel/steel contact. *Wear* 2004;256(1):44–8.
- Wessling B. Corrosion prevention with an organic metal (polyaniline): surface ennobling, passivation, corrosion test results. *Mater Corros* 1996;47(8):439–45.
- Fahlman M, Jasty S, Epstein AJ. Corrosion protection of iron/steel by emeraldine base polyaniline: an X-ray photoelectron spectroscopy study. *Synth Met* 1997;85(1): 1323–6.
- Radhakrishnan S, Siju CR, Mahanta D, Patil S, Madras G. Conducting polyaniline-nano-TiO<sub>2</sub> composites for smart corrosion resistant coatings. *Electrochim Acta* 2009;54(4):1249–54.
- Deshpande PP, Jadhav NG, Gelling VJ, Sazou D. Conducting polymers for corrosion protection: a review. *J Coating Technol Res* 2014;11(4):473–94.
- Fang J, Xu K, Zhu L, Zhou Z, Tang H. A study on mechanism of corrosion protection of polyaniline coating and its failure. *Corrosion Sci* 2007;49(11):4232–42.
- Grgur BN, Elkais AR, Gvozdenović MM, Drmanić SZ, Trisović TL, Jugović BZ. Corrosion of mild steel with composite polyaniline coatings using different formulations. *Prog Org Coating* 2015;79:17–24.
- Ohtsuka T. Corrosion protection of steels by conducting polymer coating. *Int J Corros* 2012;(5). <https://doi.org/10.1155/2012/915090>.
- Peng Y, Hu Y, Wang H. Tribological behaviors of surfactant-functionalized carbon nanotubes as lubricant additive in water. *Tribol Lett* 2007;25(3):247–53.
- Ge XY, Xia YQ, Cao ZF. Tribological properties and insulation effect of nanometer TiO<sub>2</sub> and nanometer SiO<sub>2</sub> as additives in grease. *Tribol Int* 2015;92(3):454–61.
- Cao ZF, Xia YQ. Study on the preparation and tribological properties of fly ash as lubricant additive for steel/steel pair. *Tribol Lett* 2017;65(3):104.
- Fan XQ, Wang LP, Wen L. In situ fabrication of low-friction sandwich sheets through functionalized graphene crosslinked by ionic liquids. *Tribol Lett* 2015;58(1):12.